-RESEARCH PAPER-

International Journal of Mining and Geo-Engineering

IJMGE

IJMGE 58-2 (2024) 221-227

DOI: 10.22059/IJMGE.2024.370106.595134

Maximizing of the coverage and quality in micro resistivity image log by applying minimum weighted norm interpolation and anisotropic diffusion filter

Yahya Moradi Chaleshtori [a], Saeed Yarmohammadi [a, *], Reza Mohebian [c] and Behnia Azizzadeh Mehmandost Olya [c]

[a] *Petroleum Engineering Department, Petropars LTD Company, Tehran, Iran.*

[b] *Engineering & Business Development Department, OIEC group, Tehran, Iran.*

[c] *School of Mining Engineering, College of Engineering, University of Tehran, Tehran, Iran.*

Article History:

Received: 24 December 2023.

Revised: 24 January 2024.

Accepted: 08 April 2024.

ABSTRACT

The micro-resistivity imaging log is a crucial tool for measuring the heterogeneous features of a formation. It objectively and quantitatively describes various reservoir characteristics, including fine structures, thin strata, fissures, and sedimentary facies. In these imaging tools, measurements from button arrays create an electrical image of the wellbore. However, gaps between tool pads limit coverage, and damaged buttons may compromise image quality. In this study, image log data are examined for factors impacting data acquisition, followed by processing for basic correction, image enhancement, static, and dynamic image log creation. To achieve 100% coverage, the Minimum Weighted Norm Interpolation (MWNI) algorithm fills gaps between tool pads. Finally, the Anisotropic Diffusion Filter (ADF) reduces noise and enhances image log quality in MATLAB, providing a comprehensive image from logging tools. As image logs play a crucial role in illustrating the wellbore and reservoir, this study suggests a new workflow to successfully tackle the challenges associated with acquiring comprehensive image log coverage.

Keywords: *Micro resistivity imaging log, Formation features, Minimum weighted norm interpolation, Anisotropic diffusion filter.*

1. Introduction

The micro-resistivity imager stands as a preeminent and highly valuable advanced logging tool, offering real-time micro-resistivity formation images and dip data [1,2]. This sophisticated tool operates by transmitting an alternating current from the pusher plate. As the current traverses the borehole mud column and the formation, it subsequently returns to the circuit electrode positioned at the top of the tool [3]. The reflections of resistivity changes are meticulously measured from the current intensity on the electric buttons. This nuanced interplay between current and formation micro-resistivities provides invaluable insight into the structural and electrochemical nonhomogeneity of the formation itself [4]. Following a comprehensive processing stage, the information gleaned from the electric buttons undergoes transformation, resulting in a visually informative earth-colored or grayscale image [5,6].

The versatility of borehole images extends across various realms within the geosciences. In sedimentology, image logs are crucial for the analysis of facies [7], examination of formation fabric and structure [7,8], assessment of depositional environments [9], and exploration of geological body geometry and sequence stratigraphy [10,11]. Moreover, in the domain of structural geology and geomechanics, borehole image results are indispensable for determining structural dip, fault identification, fracture characterization, and in situ stress analysis [12, 13, 14, 15]. In petrophysical studies, the interpretation of image logs plays a pivotal role in advancing reservoir characterization and conducting nuanced heterogeneity analyses [15,16].

Despite the numerous advantages associated with the use of image logs, ongoing research addresses certain limitations [3]. Frequently, the effects of hole conditions, mud types, and acquisition practices are addressed and compensated for through the application of various processing algorithms [9].

The contemporary landscape of petroleum engineering has witnessed a remarkable surge in the utilization of both intelligent and semi-intelligent methods. This heightened adoption can be attributed to the notably favorable outcomes yielded by these approaches in tasks such as data estimation, lost data reconstruction, forecasting, and the production of precise datasets. The proliferation of these methodologies has become pervasive, evident in their application across a spectrum of functions, including estimating the Q factor, computing potential permeability maps, appraising fractures, and amalgamating meta-attributes for 3D modeling [17, 18, 19, 20]. The widespread acceptance of these methods can be ascribed to their inherent capacity to produce highly accurate results. Hence, the focus of this article is to employ programming and intelligent methodologies for the reconstruction of lost data within the FMI dataset [21].

The Minimum Weighted Norm Interpolation (MWNI) method is a powerful mathematical technique widely employed in geophysics,

* Corresponding author. *E-mail address:* : mohebian@ut.ac.ir (R. Mohebian).

particularly in the domain of seismic data processing and well imaging [22,23]. Its primary purpose is to address the common challenge of incomplete or missing data points within spatial datasets. In the context of geophysics, such as seismic data acquisition, missing information can arise due to practical limitations or equipment malfunctions. MWNI steps in to fill these gaps by formulating an objective function that minimizes the difference between observed data and interpolated values at missing locations, all while incorporating a weighting scheme based on proximity to the missing points.

The key strength of MWNI lies in its mathematical foundation, grounded in principles of optimization and linear algebra. The method seeks to find solutions to underdetermined linear systems, where the number of unknowns surpasses the available equations. The term "Minimum Norm" in MWNI underscores its preference for solutions with the smallest overall magnitude, promoting smooth and coherent interpolations that minimize abrupt changes or artifacts in the reconstructed data [24]. This optimization process involves iteratively adjusting values at missing locations, assigning higher weights to points closer to the gaps, and striving for a solution that balances the observed data and any additional constraints [25].

Initially designed for the regularization of seismic data at missing spatial locations, the MWNI method has evolved and found utility in recent studies, particularly in the interpolation of prestack and poststack seismic data [26]. Recent research efforts have sought to optimize the MWNI method through integration with complementary techniques [27, 28, 24]. The Anisotropic Diffusion Filter (ADF) is another notable method employed to reduce image noise while preserving crucial content and details for interpretation [29,30]. Widely acknowledged in image processing studies, the ADF method is regarded as a systematic procedure for noise reduction and quality improvement [31, 32].

The efficacy of image log tools in covering boreholes varies, contingent upon factors such as the number of pads and borehole size, resulting in coverage percentages ranging from 30% to 80% [33]. In the present study, the MWNI method is implemented with the explicit goal of maximizing borehole coverage to an impressive 100%. This interpolation method adeptly fills the gaps between pads and flaps, yielding a fully covered borehole image that significantly enhances the reliability of interpretation. Furthermore, the study employs the ADF to eliminate all noise and misadjustments from the generated fully covered image, culminating in a high-resolution borehole image. This meticulous noise reduction process not only refines image logs but also aids interpreters in identifying and discerning reliable geological features in the context of hydrocarbon reservoir studies [34].

The main goal of this study is to suggest a new workflow that effectively overcomes challenges related to obtaining high-quality, comprehensive coverage of image logs. This consideration is based on the crucial role of image logs in visualizing the wellbore and reservoir.

2. Methodology

A practical approach to establishing a well-founded image of reservoir intervals is offered by applying a sequence of processing functions, including MWNI and ADF (Figure 1). In the following section, a concise overview of the methodologies employed on image logs is provided. These methods have been systematically applied to fulfill the objectives of this study, contributing to a comprehensive understanding of reservoir characteristics and facilitating accurate analysis.

2.1. Data Quality Assessment and Preparatory Steps for Analysis

Before delving into the analysis of microresistivity data, it is imperative to assess the data quality, particularly with regard to tool-related parameters, as these factors significantly influence both borehole survey data and image quality [35]. In this study, various data acquisition parameters, including pad pressure, gain selection, the ratio of formation to mud resistivity, logging speed, and pre-processing procedures, are meticulously examined and optimized.

Subsequently, the crucial step of generating log quality cross plots is taken, aimed at validating the accuracy of data collected by the survey tool's magnetometer and accelerometer within the logging string. These plots serve as a robust indicator of the reliability of directional information obtained from these sensors.

For the magnetometer data, an X versus Y log plot is employed, which ideally should exhibit a circular or arc distribution centered at the origin (0, 0). This distribution pattern aligns with the fact that image data is stored in a vertical well (as depicted in Figure 2).

To further validate the directional information, accelerometer data is scrutinized using the ZX and ZY quality control crossplot, as presented in Figure 3. The Z-axis accelerometer gauges the strength of the gravity field along the tool axis, accounting for both upward and downward tool movements in vertical wells. In this vertical well, the Z-axis accelerometer reads at approximately (1g = 9.81m/s² = 32.2ft/s²).

Moreover, considering the impact of borehole conditions, including washouts and variations in drill section size [30], is essential. To assess these conditions across the reservoir intervals, the borehole geometry profile derived from caliper logs is visualized, as illustrated in Figure 4.

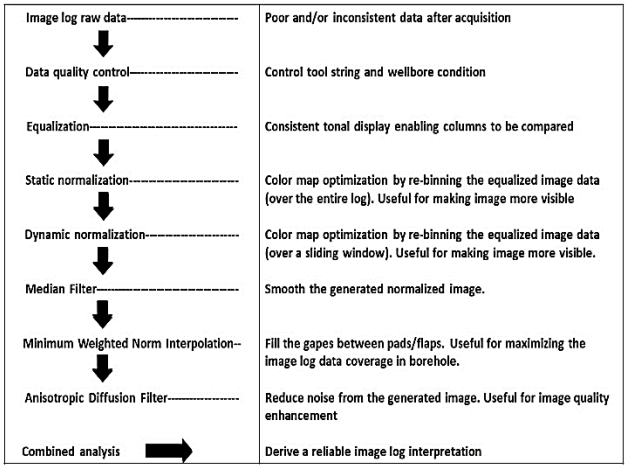

Figure 1. Schematic workflow describing the component steps in coverage and quality maximizing of image log.

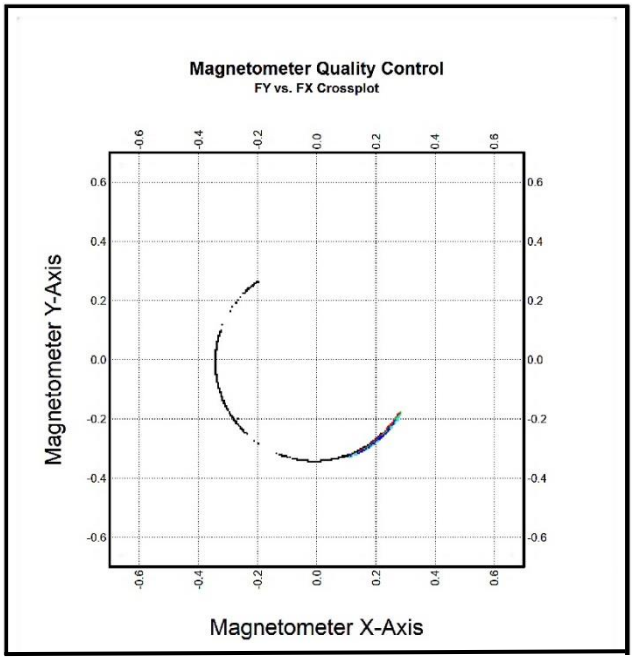

Figure 2. The magnetometer components of the image log tool (Fx vs Fy) cross plot. The arc distribution serves as confirmation that the directional information from the magnetometer is accurate.

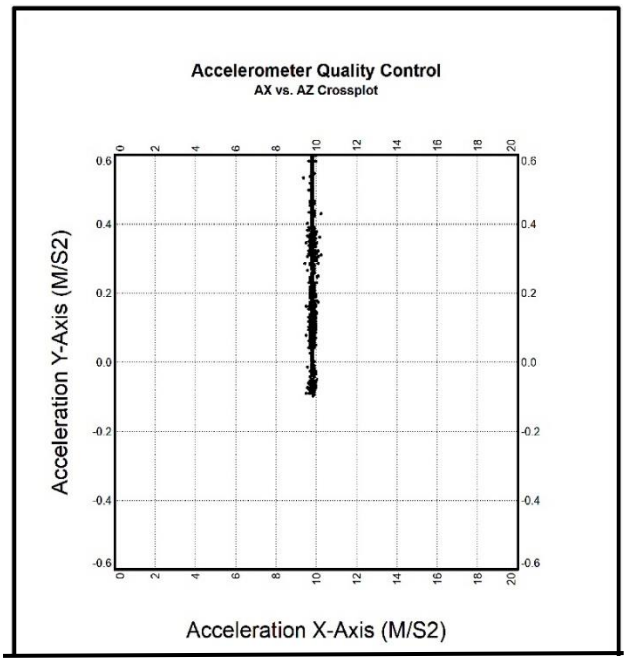

Figure 3. The accelerometer components of the image log tool (Ax vs Ay) cross plot. The arc distribution underscores the accuracy of the directional information from the magnetometer.

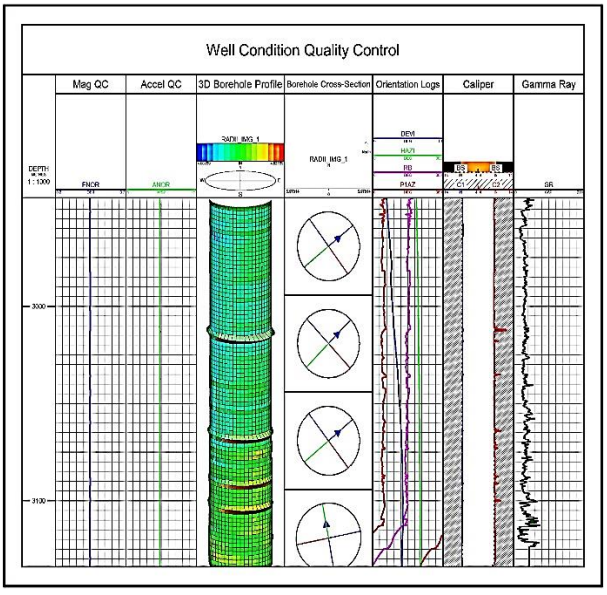

Figure4. Evaluation of borehole geometry profile and its effects on well condition and data acquisition.

Finally, as part of the quality control process, the microresistivity data recorded by various button arrays (rows) is inspected. Figure 5 demonstrates that there are no significant irregularities in the pad data, ensuring that data processing can proceed smoothly without any impediments.

This meticulous data quality assessment and preparatory phase lay the foundation for reliable and accurate analysis of microresistivity imaging logs in subsequent stages of this study.

3. Processing of FMI Data

In numerous image logs, distortions become apparent in the raw data, indicating a mismatch between cable speed and pre-processing speed. This study begins by applying a speed correction function to the raw data, specifically addressing image roughness in intervals where the tool came to a halt. Following this, image enhancement processing is conducted on the raw data through several steps, encompassing accenting correction, equalization, normalization, image filtering, and histogram upscaling. The objective is to enhance the visual quality of image logs.

Eccentering correction generates a radius and rectifies tool eccentering errors. Equalization is essential to adjust the standard deviation and mean data of each column, ensuring consistent comparability with other columns [7]. To make optimal use of the color map, a normalization module is applied to the data distribution, enhancing visibility of details by re-binning the data either statically (over the entire log) or dynamically (over a sliding window) to match a predefined frequency distribution (Figure 6) [36].

Finally, pre-defined filters such as median, Gaussian, and Laplacian are employed to smooth the image log (Figure 7). The histogram upscaling involves a sliding window traversing through a log, calculating a histogram at each step.

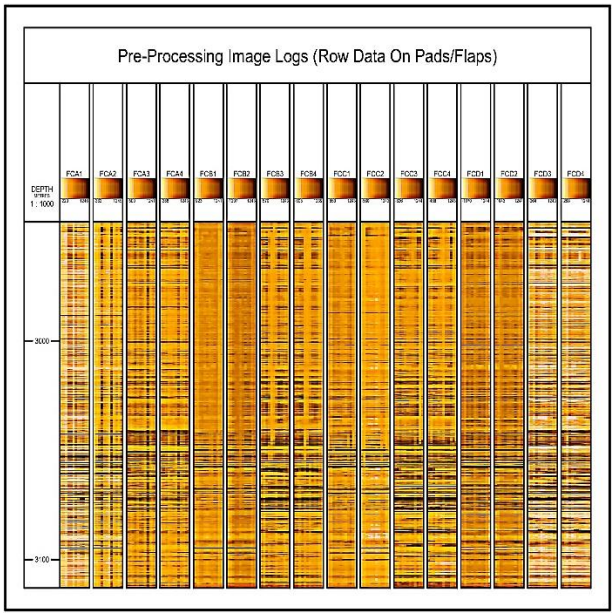

Figure5. Quality control of pad/flap raw data and comparison of microresistivity data obtained from button arrays.

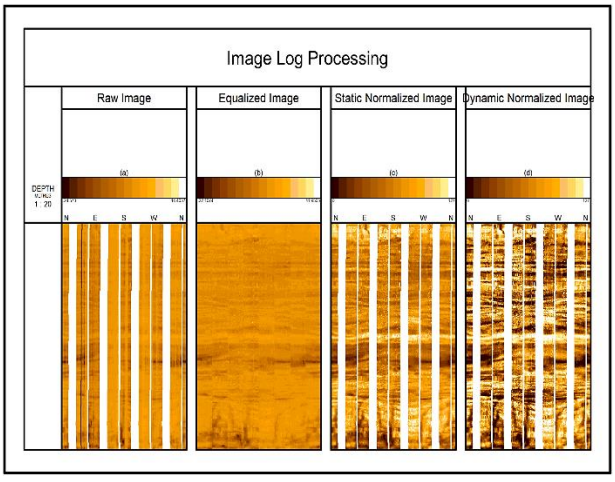

Figure 6. (a) The generated raw image log from recorded microresistivity data, (b) the adjusted image log after equalization, (c) static image log (normalized over the entire log), (d) Dynamic image log (normalized over sliding window).

4. Minimum Weighted Norm Interpolation (MWNI)

A comprehensive image log offers more realistic information about the wellbore condition in various reservoir intervals. The consistent absence of data and empty spaces in image logs indicates a deficiency in data acquisition, attributed to limitations in the tool. The challenge of signal reconstruction or interpolation using common inverse equations arises from the necessity to solve a system of underdetermined equations, where there are more unknowns than observations. This issue has multiple potential solutions, and, in general, providing relevant prior information and constraining the range of solutions would be one of the most effective approaches to address this type of problem.

One method that serves as an inversion-based solution is called minimum weighted norm interpolation (MWNI), as proposed by Liu and Sacchi in 2004. The reconstruction of data with missing samples can be summarized in the following inversion scheme, represented by Equation (1):

$$Minimize\|x\|_w^2 subject to Tx = y \quad (1)$$

In this equation, $\|.\|_w$ represents a specific weighted norm, and T is the sampling matrix that maps desired data samples (x) to available samples (y). The transpose of T is used to fill in the positions of missing samples with zeros.

The specific weighted norm used in MWNI is derived from the wavenumber-domain term, as shown in Eq. 2:

$$\|x\|w^2 = \Sigma(k \in \kappa)(x_k^* x_k)/(P_k^2) \quad (2)$$

Here, P_k^2 represents the weight of a spectral domain with a matching support and shape as the interpolated signal. The set of κ indexes defines the spectral support region of the signal, where $P_k^2 \neq 0$ for $k \in \kappa$. The coefficient P_k^2 reflects the spectral power in the wavenumber index k.

The minimum norm solution is obtained by minimizing a cost function, as described in Eq. 3:

$$J = b^T(Tx - y) + \|x\|_w^2 \quad (3)$$

In this equation, 'b' represents the Lagrangian multiplication vector. By minimizing 'J' with respect to 'x' while subject to the constraint $Tx - y = 0$, a solution is derived that allows the reconstruction of missing data.

In essence, MWNI is a powerful technique that leverages prior knowledge and wavenumber-domain information to effectively reconstruct missing data samples in image logs, providing a more comprehensive and accurate representation of wellbore conditions in various reservoir intervals.

5. Anisotropic Diffusion Filter (ADF)

The anisotropic diffusion method emerges as a highly effective solution, fulfilling the dual purpose of enhancing edges and minimizing noise in image processing. To elevate the quality of the image log for clear visualization and accurate interpretation, it becomes imperative to employ a method that diminishes noise while preserving intricate image details. To achieve this objective, the Perona-Malik model, incorporating the anisotropic diffusion algorithm, is utilized for noise removal [37]. Additionally, an edge-stopping approach is employed to enhance data quality. The utilization of an appropriate edge-stopping function ensures the clarity of small details and sharp edges (Eq. 4):

$$\partial u/\partial t = div\big(C(|\nabla u|)\big)\nabla u \quad (4)$$

In Eq. 4, $'u_t'$ represents the image obtained after a diffusion time 't,' while 'div' denotes the divergence operator, and '∇' signifies the gradient operator concerning the spatial variables 'x' and 'y.' The term '|∇|' represents the local gradient magnitude, and 'c(.)' serves as the diffusion coefficient or the edge stopping function.

The key characteristic of the edge-stopping function lies in its ability to take on a zero or negligible value for gradients corresponding to edges (Eq. 5 and Eq. 6):

$$C_1(|\nabla I|) = exp(-(|\nabla I|/2)^2) \quad (5)$$

$$C_2(|\nabla I|) = 1/(1 + (|\nabla I|/2)^2) \quad (6)$$

In this context, the parameter 'K' serves as the threshold for the gradient magnitude, playing a crucial role in influencing the diffusion rate. The Perona-Malik model, through the utilization of either of the two edge functions, adeptly preserves the sharp edges and intricate details within the denoised image.

Fundamentally, employing the anisotropic diffusion filter, particularly through the Perona-Malik model, proves to be a robust strategy for enhancing the quality of the image log. This technique not only diminishes noise but also safeguards the integrity of essential features, thereby contributing to clearer visualizations and more reliable interpretations.

6. Results &discussion

Image logs offer diverse information about carbonate and sandstone reservoirs. Through the accurate measurements of formation resistivities and conductivities, numerous structural and sedimentological features become visible after data processing (Figure 8). The clarity of the image enables geoscientists to achieve reliable formation interpretation and reservoir characterization.

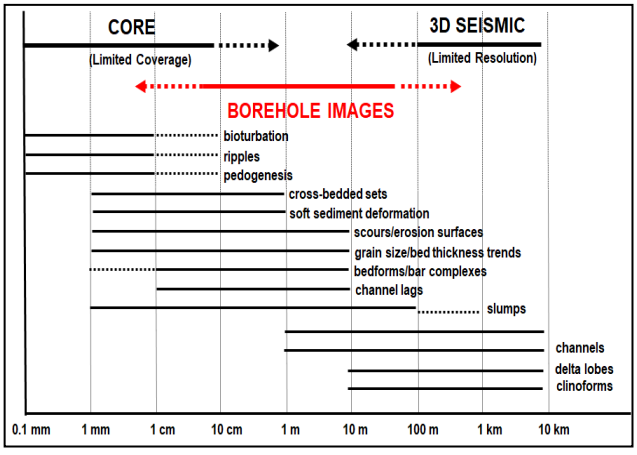

Figure 8. Scale of geological features that could be displayed in borehole images, core and 3D seismic.

In this study, Schlumberger's Fullbore Formation MicroImager (FMI) data, recorded in an 8.5-inch drilled borehole, undergoes thorough processing. The FMI is an imaging log tool capable of providing microresistivity data in wells using water-based drilling fluids. This tool consists of four arms, each equipped with a flap and pad. The image log data is recorded by an array of electrodes placed on each flap/pad (Figure 9).

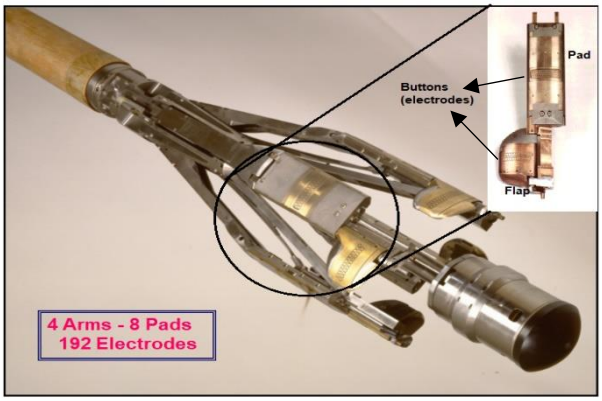

Figure 9. Schlumberger fullbore formation microimager tool (FMI).

Images of actual geological features differ from core appearances due to borehole geometry, the nature of tool measurements, well conditions, and limitations of coverage. In the framework of this study, efforts have been made to achieve maximum image quality and coverage by employing various methods, particularly novel approaches like the MWNI algorithm for optimal interpolation in image gaps and an anisotropic diffusion filter to minimize data acquisition and processing noise.

In the first step, data quality is ensured through orientation checks, magnetic declination correction, speed correction, depth matching, and the alignment of buttons, pads, and flaps. FMI data is initially loaded into Geolog software, and quality control of magnetometer and accelerometer data confirms that image log data are recorded without significant problems. Borehole conditions are then examined to understand the impact of changes in borehole diameters, particularly the presence of washouts, rugosity, and mudcake throughout the reservoir. Finally, the application of buttons in recording data is separately compared. The analysis of pad/flap data provides information about potential physical tool problems, whether intermittent, actual equipment failure, or due to changes in formation properties.

In the second step, image processing is initiated and carried out in several phases. Firstly, an image is generated in Geolog software to map all button traces and create color images of resistivity. During the image generation phase, considerations include the interpolation of curve data to form images, button equalization, and pad normalization (Figure 6). Subsequently, the quality of the generated image is enhanced through static and dynamic normalizations. A consistent color scale is applied to the entire log in static normalization, while a sliding window and histogram scaling to the middle sample are used to generate a dynamically normalized image (Figure 6). Lastly, a median filter is employed to reduce the noise in the generated dynamic image (Figure 7).

In the final steps, the array data of the dynamic image (192 microresistivity data at each depth) is imported into MATLAB software, and the MWNI algorithm is applied to traces. The algorithm successfully recovers pad/flap gap data from periodically non-uniformly spaced button array data. Figure 10 compares the amplitude of the original data with the MWNI reconstructed data, illustrating the reliability of the correlation between the reconstructed data and the values of the original processed data, indicating an approved trend for interpolated data in the gaps.

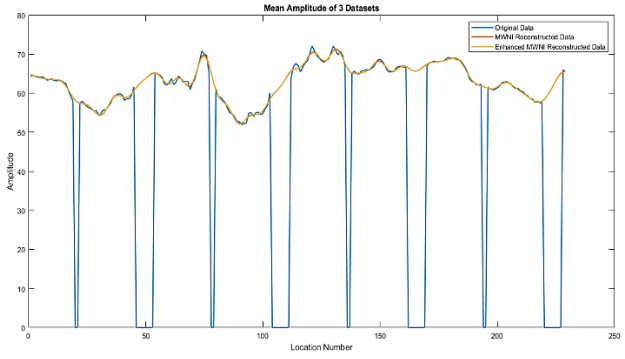

Figure 10. Comparison between the amplitude of original data and MWNI reconstructed data.

The implementation of the MWNI algorithm significantly enhances the quality of image log data, with the number of image values at each depth increasing notably, from 192 to 240. This enhancement is crucial in effectively filling the gaps between the pads and flaps of each arm, considering the mean amplitudes of the data. Consequently, there is a substantial improvement in the coverage of the borehole image, escalating from the initial 80% to a full 100% in the 8.5-inch borehole, as visually depicted in Figure 11.

Following the interpolation of missing data, the subsequent application of the Anisotropic Diffusion Filter (ADF) further contributes to refining the reconstructed image, as evidenced in Figure 11. The ADF's noise reduction process plays a crucial role in eliminating nearly all unwanted microresistivity data fluctuations received from electrodes. Additionally, it effectively smoothens out random variations in brightness or color information that may arise during the image processing and reconstruction stages.

Above all, the graphical representation in Figure 12 illustrates that the high-quality, fully covered image log can be visualized in a cylindrical shape using MATLAB software. This visualization not only provides valuable information but also proves to be comparable to core data, enhancing our understanding of subsurface formations and their intricate details.

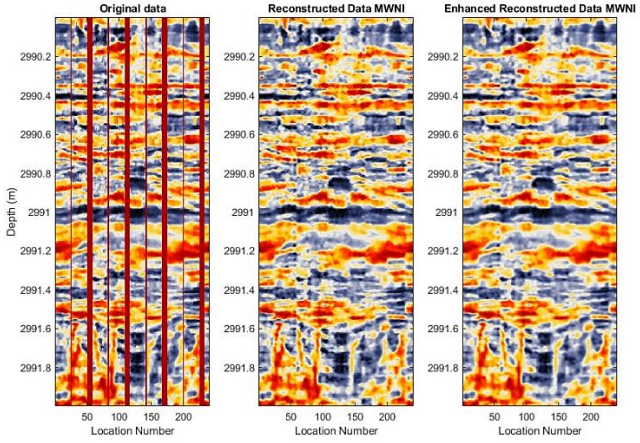

Figure 11: Image log after reconstruction and quality enhancement using MWNI and ADF method in MATLAB software.

At the conclusion of this research, the fully covered image log is imported into Geolog software for visualization and comparison with other images within a specified software environment (Figure 13). The results illustrate how the MWNI and ADF approaches enhance the quality and coverage of image logs, creating an integrated borehole image where all formation features remain constant and can be distinctly identified.

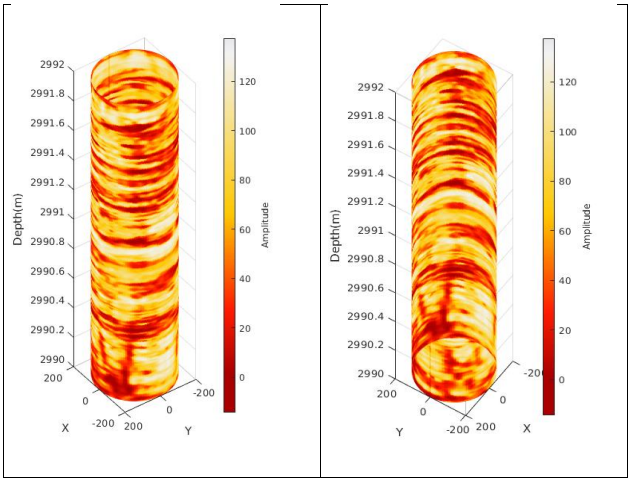

Figure 12. High quality full-covered cylindrical image logs in MATLAB software.

7. Conclusion

In this study, two approaches, MWNI and anisotropic diffusion, are delineated to improve the quality and coverage of FMI images post-processing. These techniques have demonstrated success in efficiently

interpolating data gaps between tool arms and reducing noise in the processed image logs. Following a thorough examination of data for erratic tool movements and borehole wall characteristics, the data was prepared for image processing. Subsequently, processes such as image generation, button equalization, and pad normalization were implemented to instill confidence in image analysis. Image enhancements were then applied through static normalization (using the same color scale for the entire log) and dynamic normalization, involving the consideration of sliding color scaling windows on log data.

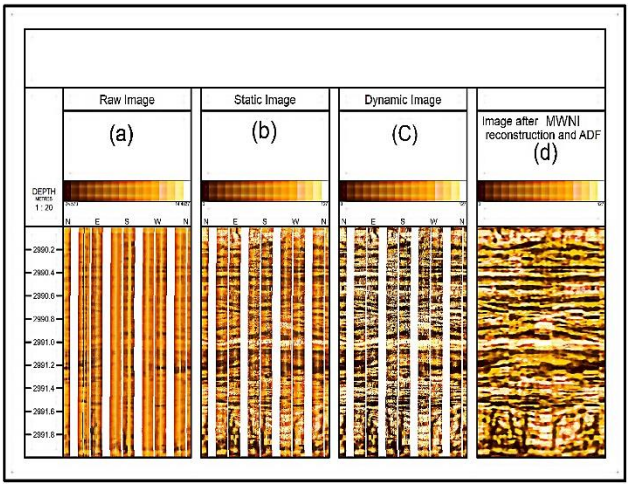

The processed data in MATLAB is subjected to the MWNI method, which serves to interpolate missing data and mitigate tool weaknesses. This dual functionality ensures not only enhanced data completeness but also refined accuracy in reservoir understanding. Furthermore, noise reduction is achieved by the anisotropic diffusion filter, contributing to clearer images and aiding in the identification of subtle features. The combined use of MWNI and ADF results in reservoir interval images comparable to core data, providing comprehensive insights for reservoir evaluation. A high-quality, fully covered image log not only speeds up image log interpretation but also makes it more cohesive, facilitating seamless integration into reservoir modeling processes. The sequential application of these techniques to image logs highlights their value in enhancing image quality and contributing to a better understanding of sedimentological and structural features, ultimately optimizing decision-making in subsurface exploration and reservoir management.

REFERENCES

[1] P. S. Cheung, "Microresistivity and ultrasonic imagers: tool operations and processing principles with reference to commonly encountered image artefacts," Geological Society, London, Special Publications, vol. 159, no. 1, pp. 45-57, 1999.

[2] C. Yuan, C. Zhou, F. Zhang, S. Hu and C. Li, "A novel method for quantitative geosteering using azimuthal gamma-ray logging," Appl Radiat Isot, vol. 96, pp. 63-70, 2015.

[3] . K. A. Safinya,, p. Le Lan, M. Villegas, and P. S. Cheung, "Improved formation imaging with extended microelectrical arrays," in In SPE Annual Technical Conference and Exhibition?, 1991.

[4] M. Ahmadi, Use of micrologs and electrical borehole images for fracture detection, natural buttes field, Uinta Basin, Utah, Doctoral dissertation, Colorado School of Mines, 2006.

[5] W. U. Hong-xia, X. I. E. Yun and Q. I. U. Yi-gang, "Application of FMI imaging logging to interpretation of sedimentary facies in Lijin Sub-Sag," Xinjiang Petroleum Geology, vol. 29, no. 6, p. 765, 2008.

[6] M. Mirzakhanian and H. Hashemi, "Semisupervised fuzzy clustering for facies analysis using extended elastic impedance seismic attributes," Geophysics, vol. 87, no. 4, pp. N75-N84, 2022.

[7] S. Yarmohammadi, D. A. Wood and A. Kadkhodaie, "Reservoir microfacies analysis exploiting microscopic image processing and classification algorithms applied to carbonate and sandstone reservoirs," Marine and Petroleum Geology, vol. 121, p. 104609, 2020.

[8] G. Aghli, R. Moussavi-Harami and R. Mohammadian, "Reservoir heterogeneity and fracture parameter determination using electrical image logs and petrophysical data (a case study, carbonate Asmari Formation, Zagros Basin, SW Iran)," Petroleum Science, vol. 17, pp. 51-69, 2020.

[9] C. Li, X. Li and Z. Liu, "Image Segmentation Process Algorithm And Its Application In Vuggy Reservoir Interpretation," in SPWLA Annual Logging Symposium, 2009.

[10] W. Utomo, A. Suleiman, A. Bachtiar, B. Satrio and A. Kartiyanta, "High Resolution Sequence Stratigraphy of," 2014.

[11] I. Ferreira, L. Ochoa and A. Koeshidayatullah, "On the generation of realistic synthetic petrographic datasets using a style-based GAN," Sci Rep, vol. 12, no. 1, p. 12845, 2022.

[12] Z. Zeng and A. Jiang, "Geomechanical study of Bakken Formation for improved oil recovery," ISRM SINOROCK, 2009.

[13] M. Hozayen, E. S. Radwan,, X. Zhang,, P. Nawrocki and A. Jebbouri, "Geomechanical Study of Fractured Carbonate Reservoir–Part II, 3D Wellbore Stability Analysis and FMI Image Logs Calibration," in 13th ISRM International Congress of Rock Mechanics, 2015.

[14] T. Dasgupta, S. Dasgupta and S. Mukherjee, "Image Log Interpretation and Geomechanical Issues. Teaching," Teaching Methodologies in Structural Geology and Tectonics, pp. 237-251, 2019.

[15] R. Baouche, S. Souvik and B. Khadidja, "Present day In-situ stress magnitude and orientation of horizontal stress components in the eastern Illizi basin, Algeria: A geomechanical modeling," Journal of Structural Geology, vol. 132, p. 103975, 2020.

[16] W. Bawazer, A. Lashin and M. Kinawy, "Characterization of a fractured basement reservoir using high-resolution 3D seismic and logging datasets: A case study of the Sab'atayn Basin, Yemen," PLoS One, vol. 13, no. 10, 2018.

[17] B. Azizzadeh Mehmandost Olya and R. Mohebian, "Hydrocarbon reservoir potential mapping through Permeability estimation by a CUDNNLSTM Deep Learning Algorithm," International Journal of Mining and Geo-Engineering, 2023.

[18] B. Azizzadeh Mehmandost Olya and R. Mohebian, "Q-FACTOR ESTIMATION FROM VERTICAL SEISMIC PROFILING (VSP) WITH DEEP LEARNING ALGORITHM, CUDNNLSTM," JOURNAL OF SEISMIC EXPLORATION, vol. 32, pp. 89-104, 2023.

[19] S. Kelishami, R. Mohebian and O. Salmian, "A comprehensive perspective on pore connectivity and natural fracture analysis in Oligo-Miocene heterogeneous carbonates, southern Iran," Journal of Petroleum Science and Engineering, vol. 208, p. 109199, 2022.

[20] M. Hosseini, M. Riahi and R. Mohebian, "A Meta attribute for reservoir permeability classification using well logs and 3D seismic data with probabilistic neural network.," Bollettino di Geofisica Teorica ed Applicata, vol. 60, no. 1, 2019.

[21] B. Azizzadeh Mehmandost Olya, R. Mohebian, H. Bagheri, A. Mahdavi Hezaveh and A. KhanMohammadi, "Toward Real-time Fracture Detection on Image Logs Using Deep Convolutional Neural Networks, YoloV5," Interpretation, pp. 1-47, 2024.

[22] S. Chiu, "Multidimensional interpolation using a model-constrained minimum weighted norm interpolation," Geophysics, vol. 79, no. 5, pp. V191-V199, 2014.

[23] J. Choi, Y. Song, J. Choi, J. Byun, S. Seol and K. Kim, "Trace Interpolation using Model-constrained Minimum Weighted Norm Interpolation.," Geophysics and Geophysical Exploration, vol. 20, no. 2, pp. 78-87, 2017.

[24] X. Pan, S. Zu, F. Gong and S. Cao, "A fast minimum weighted norm interpolation," SEG Technical Program Expanded Abstracts, pp. 4107-4111, 2016.

[25] H. Rauhut and W. Rachel, "Interpolation via weighted ℓ1 minimization," Applied and Computational Harmonic Analysis, vol. 40, no. 2, pp. 321-351, 2016.

[26] B. Liu and M. D. Sacchi, "Minimum weighted norm interpolation of seismic records," Geophysics, vol. 69, no. 6, pp. 1560-1568, 2004.

[27] M. D. Sacchi and B. Liu, "Minimum weighted norm wavefield reconstruction for AVA imaging," Geophysical Prospecting, vol. 53, no. 6, pp. 787-801, 2005.

[28] S. K. Chiu, "Multidimensional interpolation using a model-constrained minimum weighted norm interpolation," Geophysics, vol. 79, no. 5, pp. V191-V199, 2014.

[29] C. Palma, F. Cappabianco, J. Ide and P. Miranda, "Anisotropic diffusion filtering operation and limitations-magnetic resonance imaging evaluation," IFAC Proceedings, vol. 47, no. 3, pp. 3887-3892, 2014.

[30] G. Vasu and P. Palanisamy, "Multi-focus image fusion using anisotropic diffusion filter.," Soft Computing, vol. 26, no. 24, pp. 14029-14040, 2022.

[31] J. Xu, Y. Jia, Z. Shi and K. Pang, "An improved anisotropic diffusion filter with semi-adaptive threshold for edge preservation," Signal Processing, vol. 119, pp. 80-91, 2016.

[32] E. Cuevas, H. Becerra and A. Luque, "Anisotropic diffusion filtering through multi-objective optimization.," Mathematics and Computers in Simulation, vol. 181, pp. 410-429, 2021.

[33] A. Shahinpour, "Borehole image log analysis for sedimentary environment and clay volume interpretation," (Master's thesis, Institutt for petroleumsteknologi og anvendt geofysikk)., 2013.

[34] Z. M. Zhu, J. S. Shen and H. Yu, "Noise removal and fracture analysis in borehole images using mathematical morphology and compressive sensing," in 78th EAGE Conference and Exhibition 2016, 2016.

[35] M. Poppelreiter, C. Garcia-Carballido and M. Kraaijveld, Dipmeter and borehole image log technology, vol. 92, AAPG, 2010.

[36] C. Zhao, Z. Qu, X. Jiang and Y. Tu, "Content-Adaptive Auto-Occlusion Network for Occluded Person Re-Identification," IEEE Trans Image Process, pp. 4223-4236, 2023.

[37] Y. Hu, X. Zhang, D. Li and W. Li, "Anisotropic diffusion filters for flow-dependent variational data assimilation of sea surface temperature," Ocean Modelling, p. 102233, 2023.

[38] T. Ye, A. Chen, C. Niu, Q. Wang and M. Hou, "Characteristics, controlling factors and petroleum geologic significance of fractures in the Archean crystalline basement rocks: A case study of the South Jinzhou oilfield in Liaodong Bay depression, North China.," Journal of Petroleum Science and Engineering, vol. 208, p. 109504, 2022.

[39] S. D. Cabrera and T. W. Parks, "Extrapolation and spectral estimation with iterative weighted norm modification," IEEE Transactions on Signal Processing, vol. 39, no. 4, pp. 842-851, 1991.

[40] X. Pan, S. Zu, F. Gong and S. Cao, "A fast minimum weighted norm interpolation," in SEG Technical Program Expanded Abstracts 2016, Society of Exploration Geophysicists, 2016.

[41] J. Weickert, "Anisotropic diffusion in image processing," Stuttgart: Teubner., 1998.

[42] J. Yu, Y. Wang and Y. Shen, " Noise reduction and edge detection via kernel anisotropic diffusion," Pattern Recognition Letters, vol. 29, no. 10, pp. 1496-1503, 2008.